



Atmospheric moisture supersaturation in the near-surface atmosphere at Dome C, antarctic plateau

Christophe Genthon¹, Luc Piard¹, Etienne Vignon², Jean-Baptiste Madeleine³, Mathieu Casado⁴,

5 Hubert Gallée¹

¹ CNRS, LGGE, Grenoble, France

² Université Grenoble Alpes, LGGE, Grenoble, France

³ LMD – IPSL, UP6 – CNRS, Paris, France

10 ⁴ LSCE – IPSL, CEA-CNRS-UVSQ-U. paris-Saclay, Gif-sur-Yvette, France

Corresponding authors: Christophe Genthon, Laboratoire de Glaciologie et Géophysique de
l'Environnement, 54 Rue Molière, BP96, 38402 Saint Martin d'Hère Cedex, France. Email:
Christophe.genthon@univ-grenoble-alpes.fr.



Abstract. Supersaturations in the natural atmosphere are frequent at the top of the troposphere where cirrus clouds form, but are very infrequent near the surface where the air is generally warmer
15 and laden with liquid and/or ice condensation nuclei. An exception is the surface of the high antarctic plateau. One year of atmospheric moisture measurement at the surface of Dome C on the East Antarctic plateau is presented and compared with results from 2 models implementing cold microphysics parametrizations: the European Center for Medium-range Weather Forecasts through its operational analyzes, and the Model Atmosphérique Régional. The measurements are obtained
20 using commercial hygrometry sensors modified to allow air sampling without affecting the moisture content even in case of supersaturation. Supersaturations are very frequent in the observations and in the models, but the statistical distribution differs both between models and observations and between the 2 models, leaving much room for improvements in both models. Unadapted hygrometry sensors generally fail to report supersaturations, and most reports of atmospheric moisture on the
25 antarctic plateau are thus likely biased low. This is unlikely to strongly affect estimations of surface sublimation because supersaturations are more frequent as temperature is lower, and moisture quantities and thus water fluxes are very small anyway. Ignoring supersaturation may be a more serious issue when considering water isotopes, a tracer of phase change and temperature, largely used to interpret snow and ice samples from the antarctic plateau and reconstruct past climates and
30 environments from ice cores. Longer and more continuous in situ observation series to test parameterizations of cold microphysics, such as those used in the formation of cirrus clouds in climate models, can be obtained at surface levels than higher in the atmosphere.

35 *Keywords:*

Antarctic plateau

Atmospheric supersaturation



Atmospheric modeling

Cold microphysics

40 *Hygrometer*

In situ measurement



1. Introduction

Ice supersaturation is frequently found in the upper troposphere [Spichtinger et al. 2003] and
45 specific cloud microphysics parameterizations are developed to represent this process in
meteorological and climate models. These models have to be validated against the observations to
reproduce cirrus and other clouds including contrails which develop at altitudes where
supersaturations occur (e.g. Rädcl and Shine [2010]). Radiosondes provide snapshot information
but obtaining in situ observation series to calibrate and validate such parameterizations is a
50 challenge because it requires flying and operating instruments on high altitude aircrafts or balloons.
Sampling supersaturated air parcels without affecting the air moisture content is also a challenge, as
the excess moisture with respect to saturation tends to condensate on any surfaces including those
of the sampling device and the sensor itself. There are thus not many in situ observations available
to characterize and quantify natural supersaturations and their evolution in time, and evaluate and
55 validate microphysics parameterizations in such conditions.

While they are frequent at high altitude, ice supersaturations do not generally occur in the surface
atmosphere, where operating instruments is obviously much easier. Conditions close to the
tropopause are however found over the antarctic ice sheet both in terms of temperature and
60 humidity levels. Because of the distance from the nearest coasts and the high elevation, the antarctic
plateau is also particularly secluded from sources of aerosols. This is the most likely place on Earth
to observe ice supersaturation in the near surface atmosphere. For instance, Schwerdtfeger [1970]
reports on observations of relative humidity with respect to ice exceeding 120% at Vostok station in
the heart of Antarctica.

65

The possibility of surface atmospheric supersaturation on the antarctic plateau raises an important



issue, that of the relative contribution of the different terms of the surface mass balance of the antarctic ice sheet. The terms are precipitation (positive for the surface) and evaporation/sublimation (negative or positive), and possibly blowing snow (positive or negative as
70 blown snow redeposits, but generally negative because of enhanced snow evaporation). Melting and runoff do not occur on the antarctic plateau and can be excluded. The net surface mass balance, observed using glaciological methods, is very small on the antarctic plateau. It is typically a few cm water equivalent per year [Arthern et al., 2006]: the antarctic plateau is one of the driest places on Earth. This is because it is so cold, and thermodynamics imply that the various terms of the surface
75 mass balance are bound to be correspondingly small. Because they are so small, and because of a harsh environment, the direct determination of precipitation and evaporation/sublimation on the antarctic plateau is not conclusive. Their relative contribution to the surface mass balance of the antarctic plateau is still poorly quantified, using indirect approaches [Frezzotti et al., 2004]. In most places on continents, precipitation largely dominates. This is not necessarily the case on the
80 antarctic plateau. In particular, if atmospheric supersaturation occurs near the surface, then moisture concentration is likely larger in the surface atmosphere than at the snow surface and the turbulent moisture flux is thus directed towards the surface (surface condensation). Unlike most other regions of the Earth, this turbulent flux could contribute positively to the surface water budget and thus, here, on the surface mass balance.

85

Another potential issue with ice supersaturation on the antarctic plateau is that of the impact on the water isotopic composition of snow. Supersaturation leads to kinetic fractionation of the stable isotopic composition of water when it condensates. Since the 1980's [Jouzel et al. 1987], the longest ice core records of past climate and environment are obtained from drilling operations on the
90 antarctic plateau. Past atmospheric temperatures are deduced from the variations of the concentration of stable water isotopes along the core. Variations in supersaturation levels may



impact on this reconstruction. Supersaturations thus involve not only meteorological (clouds, precipitation, surface evaporation / sublimation) but also climate and paleoclimate reconstruction issues. It is therefore important to measure and assess supersaturations on the Antarctic plateau.

95

However, as already mentioned, measuring atmospheric supersaturation is a challenge because sampling a supersaturated air mass can affect its moisture content. Schwerdtfeger [1970] expresses concerns about the reliability of reports of supersaturation at Vostok station. On the other hand, many reports of relative humidity with respect to ice (RH_i) on the antarctic plateau reach but seem to be capped at 100% [King et al., 1999]. Genthon et al. [2013] compare RH_i observed at Dome C on the antarctic plateau using conventional solid state sensors with results from the ECMWF (European Center for Medium-range Weather forecasts) meteorological analyzes and from the MAR (Modèle Atmosphérique Régional, Gallée and Gorodetskaya [2010]) meteorological model. In both models, cold microphysics parameterizations are used which, depending on local conditions, allow for supersaturations. More often than not, when ~100% RH_i is observed at Dome C with conventional instruments (not adapted to sample supersaturation), both models produce significant supersaturation, occasionally reaching more than 150% [Genthon et al., 2013]. The cold microphysics parameterizations differ in the 2 models (see Genthon et al. [2013] for references), and other aspects such as the vertical resolution also differ: if both model produce significant supersaturations, they do not quantitatively agree as to the amplitude of the supersaturations.

To verify such numbers and decide between models, using direct is situ measurements, instruments must be designed and/or adapted so as to bring the air mass to the moisture sensor without affecting its moisture content. This can be done by warming the air above its condensation temperature before ushering it to the sensor. Here, after the present general introduction (Section 1), Section 2 presents 2 instruments which are adaptations of commercial sensors to perform in very cold

115



conditions and to enable the measurement of atmospheric supersaturation at Dome C. The measurement site and deployment are also described in Section 2, and previous atmospheric humidity reports from this site are reminded. In Section 3, results from the older instruments are compared with the reports by the 2 adapted instruments. In this Section the models are shown to agree with the observations from the adapted instruments, of frequent occurrences of supersaturation at all time in the year including in summer. It is also shown that details of the climatology and the statistics of occurrence of supersaturation differ between the models and the observations and between the 2 models. Section 4 discusses the results, provides an outlook of research to follow, and finally concludes the paper.

2. Measurement site, instruments and methods

Dome C (Figure 1) is one of the main domes on the east antarctic plateau. Since 2005, the summit of the dome (75° 06' S, 123° 20' E, 3233 m a.s.l.) hosts a permanently manned station, Concordia, jointly operated by the French and Italian polar institutes (IPEV and PNRA). One of the first Antarctic Meteorological Research Center automatic weather station (AMRC AWS, <https://amrc.ssec.wisc.edu/>) deployed in Antarctica, back in the 1980s, was at Dome C. When the actual location of the summit of the dome was later more accurately determined using satellite and aircraft radar altimeters in the 1990s, the AWS was moved about 50 km to its present position. This induced a 30 m rise and correspondingly slight mean surface pressure change but otherwise little impacted the series consistency because the local environment is very homogeneous. The AWS provides one of the longest quasi-continuous meteorological reporting on the high antarctic plateau. The station measures pressure, temperature and wind, but not moisture. Additional meteorological reports are available since the construction of Concordia station, including an other AWS closer to the station and a daily radiosonde. Both the new station and the radiosondes report atmospheric



humidity using solid state film capacitive sensors [Kämpfer et al., 2013], . In early 2008, a system to vertically profile the lower part of the atmosphere was deployed along an ~45 m high tower. Temperature, wind and moisture are measured, the latter again using solid state film capacitive
145 sensors. This profiling system is fully described in Genthon et al. [2010], Genthon et al. [2011] and Genthon et al. [2013].

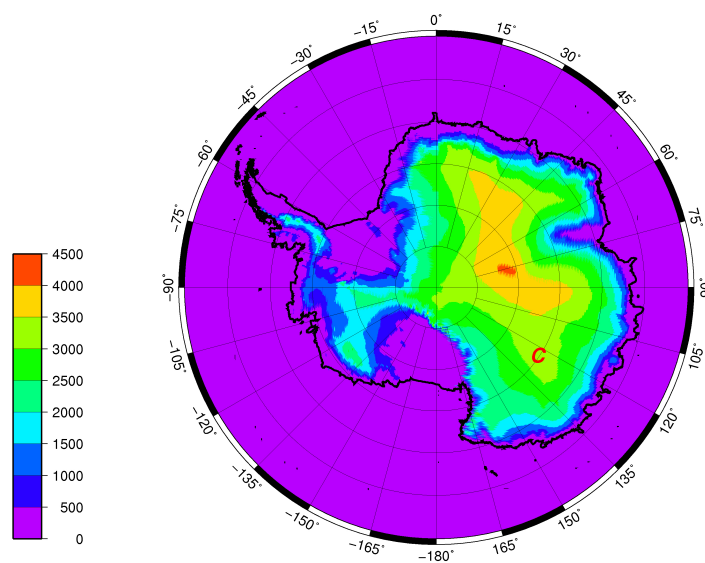


Figure 1: Topographic map of Antarctica, showing the location of Dome C (red C). Altitude” is in
m.

150

Genthon et al. [2013] evaluate and compare 2 contrasted years, 2009 and 2010, respectively the warmest and coldest in a 10-year period. They report measuring humidity up to ~100% with respect to ice but also observing frequent frost deposition, a hint that supersaturation occurs but is
155 missed by standard hygrometers without an adaption. Occurrences of supersaturation are further supported by a comparison with models that implement cold microphysics parameterizations: the



models often simulate supersaturation when the hygrometers hit the 100% RH ceiling. That raw solid state hygrometers cannot measure supersaturation is understandable: a supersaturated air mass will deposit its excess moisture on any hard surface that serves as a condensation surface. The
160 hygrometer body itself will condensate the excess moisture before it can be measured. One way to overcome this problem is to aspirate and warm the air above its thermodynamic saturation temperature at the intake.

There are several techniques to measure atmospheric moisture [Kämpfer, 2013]. The
165 traditional wet bulb thermometer is not very practical, particularly when measuring well below freezing temperature. The dew-point hygrometer provides a direct physical measure of the saturation temperature. This is done by progressively cooling from ambient temperature a surface until atmospheric moisture condensation is detected on the surface. The cooled surface is generally a mirror and condensation is optically detected when the reflection of a light beam is observed to be
170 diffused and diffracted. The device also works below freezing temperature but should then be referred as frost-point hygrometer [King and Anderson, 1999]. Dew and frost-point hygrometers are accurate but bulky, complex and expensive. They require significant amounts of energy, and they have moving parts as the mirror must be periodically cleaned. They are thus comparatively prone to dysfunction and failures, and they cannot be used in remote unattended places or in radiosondes. On
175 the other hand, they mechanically aspirate air to the sensing mirror, and if the aspiration intake is heated significantly above ambient temperature the measured air is sampled without affecting its moisture content even if supersaturated. Some commercial instruments ensure this such as the Meteolobor VTP6 Thygan described below.

180 In the 1970s, Vaisala Oy (Finland) developed a very different, very compact humidity sensor, the Humicap thin film capacitive sensor¹. The dielectric properties and capacitance of a

¹ <http://www.vaisala.com/Vaisala%20Documents/Technology%20Descriptions/HUMICAP-Technology-description->



polymer film vary with the relative humidity of the ambient air. Although the physical processes for dependence have been described (e.g. Anderson [1994]), the relationship between capacitance and atmospheric moisture is an empirical one. The sensor needs calibration and a small but significant
185 uncertainty affects the measurement. The uncertainty increases as temperature decreases. On the other hand, the Humicap is convenient, very compact, comparatively inexpensive, robust, and its use can be automated and deployed even in remote places and on radiosondes. It is thus currently widely used for such purposes. Thin film capacitive sensors are used in all automatic weather stations in Antarctica that report moisture as well as on the 45-m profiling system at Dome C
190 mentioned above, in the latter case bundled in Vaisala HMP155 thermometers – hygrometers (thermohygrometers) [Genthon et al 2013]. According to the manufacturer, the uncertainty is +/- 1.4% of the reading in the -60°C to -20°C temperature range. It may be expected to be larger below -60°C. However, then, the absolute moisture content of the atmosphere is smaller and absolute measurement errors are correspondingly smaller.

195

To tentatively confirm and quantify supersaturations at Dome C, both frost-point and thin film capacitive hygrometers were deployed at a height of 3 m and adapted as necessary to operate in the general Dome C conditions and to sample the air without altering its moisture content even when above saturation. In both systems, the hygrometer aspirated intake is heated so that the temperature
200 of the sampled air parcel is raised above condensation level and condensation is avoided. The frost-point hygrometer is a Meteolabor VTP6 Thygan chilled mirror instrument. It was selected because it is factory-designed to perform to cold temperatures and correspondingly low specific humidities. According to manufacturer the lowest measurable frost point temperature is -65°C. The fact that the air intake is heated (see below) does not improve the temperature range of the instrument as the
205 actual limitation is due to the ability to cool the mirror to the condensation temperature. A -65°C

B210781EN-C.pdf?utm_campaign=CEN-TIA-G-Humidity%20Nurturing
%202015&utm_medium=email&utm_source=Eloqua&utm_content=CEN-TIA-G-HUMICAP%20Technology
%20Promotion

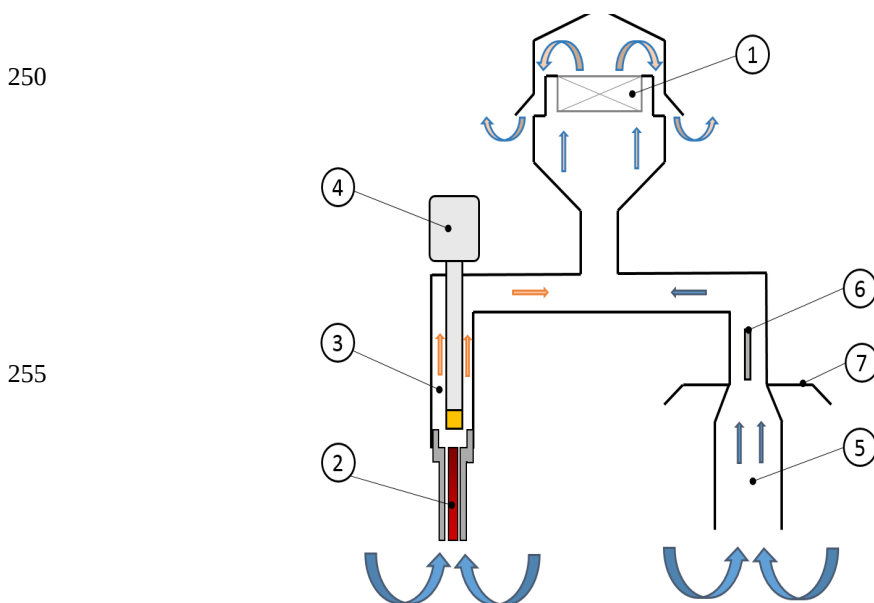


temperature limit is not quite low enough to consistently operate at Dome C, where the surface atmospheric temperature can occasionally fall below -80°C . However, data from the vertical profiling system show that from 2009 to 2015, the air temperature ~ 3 m above the snow surface was warmer than -55°C more than 50% of the time, and almost consistently (more than 99.5% of the time) warmer than -55°C during the local summer (Dec – Jan – Feb). Assuming near saturation, the instrument can nominally operate a large fraction of the time at Dome C. For our application, the frost-point hygrometer (noted FP from now on) is hosted in a heated box so that the electronics and mechanics are not affected by the extreme cold temperatures in winter. By factory design, the outside air is aspirated inside the instrument through a heated intake which prevents frost deposition. This design is not modified, the intake being simply made to protrude out of the heated box to sample the outside air. This is the only part of the instrument kept outside the heated box and, because it is itself heated, loss of moisture along the way to the mirror is consistently prevented. Visual inspection confirms that even when frost deposition occurs on other instruments on the tower, no frost deposition is observed in the vicinity of the instrument intake. Each measurement cycle lasts 10 minutes: heating and defrosting the mirror from the previous measurement, cleaning, then cooling until frost point is reached. The sensor thus reports measurements of frost point temperature, and conversion to relative humidity, on a 10' time step basis. The manufacturer claims a very high accuracy: 0.1% expressed in term of relative humidity. Dew and frost point hygrometers are indeed often used to calibrate other types of hygrometers. Here the FP is used as a reference against which other sensors may be adjusted and are evaluated, at least down to temperatures where the FP performs well.

For the other type of hygrometer used here, the manufacturer (Vaisala Oy) guarantees its HMP155 sensor down to -80°C for the measurement of temperature, but only to -60°C for the measurement of moisture. However, the main issue with colder temperatures for this instrument is that the time



response increases. Yet, unlike in a radiosonde for which the environment quickly varies during ascent, variations are comparatively slow for fixed instruments and the operational limit is actually much below -60°C [Genthon et al., 2013]. In addition, to avoid frost deposition and preserve the air moisture content, for our application, the instrument aspirates the air through an inlet consistently
235 heated $\sim 5^{\circ}\text{C}$ above the ambient temperature (Figure 2). The ambient temperature itself is measured by a separate PT100 platinum resistance thermometer in an unheated derivation of the system. A comparison with the frost point hygrometer shows that this simple and low cost innovative design succeeds to measure even highly supersaturated air, up to 200% with respect to ice or even more. In addition, the fact that the air reaching the hygrometer sensor is 5°C above ambient temperature
240 correspondingly extends the actual nominal temperature range of the instrument with respect to ambient temperature. The sensor reports relative humidity. According to manufacturer, the accuracy in the low temperature range (-60° to -40°C) is $\pm 1.4\%$ of the reading. Accuracy improves at warmer temperature, and may conversely be expected to deteriorate for even colder temperatures. The temperature range -40° to -60°C is typical at Dome C although temperatures as cold as -80°C
245 and as warm as -15°C may be encountered. Note that, in accordance with meteorological conventions, all sensors report relative humidity with respect to liquid water rather than ice even when the air temperature is below 0°C . Here the Goff-Gratch formulas [Goff and Gratch, 1946] are used to convert between RH with respect to liquid, water vapor partial pressure and RH_i.





260

Figure 2: Schematic drawing of the modified (HMPmod) hygrometer. The air is aspirated by the fan (1) and heated through an inlet (2). The temperature and the moisture content of the heated air (3) is measured by the HMP155 (4). The ambient air temperature (5) is measured by a separate PT100 (6) located in the unheated aspirated inlet shaded from sun radiation (7).

265

The 2 adapted instruments are deployed side by side ~3 m above the snow surface on the ~45-m tower. At the same level, hosted in an aspirated but unheated radiation shield (see Figure 1 of Genthon et al. [2011]), an unmodified HMP155 allows for comparison with a traditional design – and to exhibit biases of the latter. From now on, the original and modified HMP155 will be referred to as “HMP” and “HMPmod”, respectively. Table 1 lists the instruments and adaptations. The various instruments performed over the duration of 2015 except for limited periods due to datalogging failures or servicing in summer. The results are presented and analyzed in the next section.

275

Short name	Instrument / sensor	Housing
HMP	Vaisala HMP155 thermohygrometer / thin film polymer hygrometer	Aspirated radiation shield
HMPmod	Modified Vaisala HMP155 thermohygrometer / thin film polymer	Aspirated radiation shield + heated intake (Figure 2)



	hygrometer	
FP	Meteolabor Thygan VPT6 mirror frost-point hygrometer	Heated enclosure, heated intake

Table 1: List of hygrometers and adaptation. See text for details

280

3. Data, results and comparison with meteorological analyses and model simulation

3.1. Summer

285 Figure 3 displays the mean diurnal cycle of atmospheric moisture and temperature in January, February and December 2015 according to the various instruments. During this period, the FP is consistently running within its nominal manufacturer-stated temperature range and can serve as a moisture measurement reference for the other instruments. The sun never really sets at this time of the year, however its changing elevation above the horizon induces a strong temperature cycle near
290 the surface (figure 3.d). Here, “night” will broadly refer to the local hours during which sun elevation is lower at Dome C and sets at lower latitudes. Figure 3a shows the mean cycle of partial pressure of water vapor from FP. The numbers are low due to the cold temperature: the water partial pressure ranges on average between ~15 Pa in the early morning and slightly over 35 Pa in the early afternoon. This cycle demonstrates that surface evaporation occurs during the day, followed by
295 deposition at night, resulting in surface (3-m) atmospheric moisture diurnally changing by a factor of more than 2. Figure 3.b shows small differences and consistent agreement between the HMPmod and FP instruments. Note here that HMPmod is slightly calibrated for moisture report against the FP instrument for agreement in the early afternoon at the warmest of the day. This calibration does not exceed manufacturer stated accuracy for HMP155 (Section 2). The calibration proves robust and



300 valid at all time during the day in this period. Results from (unmodified) HMP significantly depart
from those of the FP, and thus HMPmod instruments: the agreement is good in the afternoon only
but quite poor the rest of the day and at night. Figure 3c displays the calculated RH_i for the 3
instruments, using the independent moisture measurements by each instrument ,but all finally
reported to the atmospheric temperatures of the (unmodified) HMP. This is likely the most accurate
305 estimation of temperature, i. e. the least likely affected by radiation and other biases because it is
unheated and efficiently ventilated [Genthon et al. ,2011]. Temperature differences of as much as
2°C are occasionally observed with the other instruments in low wind conditions.

RH_i differs markedly between the unmodified HMP and the 2 other instruments. The latter both
310 report RH_i significantly exceeding 100% while the unmodified instrument hardly reaches
saturation. All instruments agree well in the early afternoon at the warmest of the day but HMP
disagrees at night. The FP and HMPmod instruments consistently agree with each other, including
when reporting supersaturations reaching 120 % at night, confirming the high levels of
supersaturation hinted by Genthon et al. [2013] from models.

315

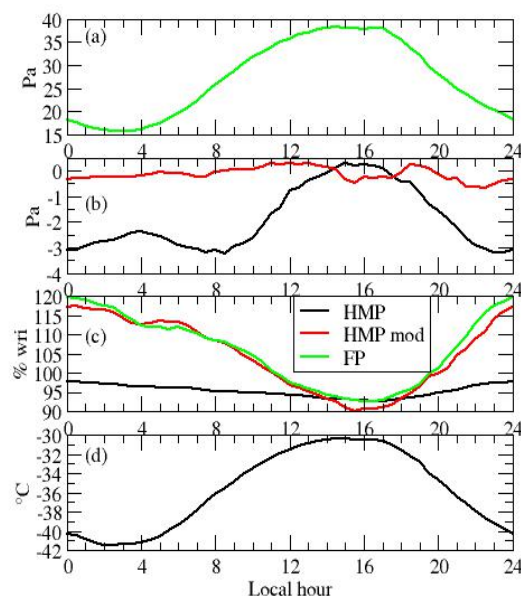


Figure 3: Mean Dec-Jan-Feb diurnal cycle of: (a) water vapor partial pressure from FP instrument
; (b) difference with respect to FP of water vapor partial pressure from original (HMP, black) and
320 modified (HMPmod, red) thin rilm polymer sensors ; (c) RH_i from the 3 instruments; (d) air
temperature.

Figure 4 compares the observed diurnal cycles of temperature and moisture with ECMWF analyses
of temperature and moisture at the 1st model level and at the standard 2 m level. The mean elevation
325 of the 1st model level in summer is 8.2 m. Thus the elevations of the 2-m and 1st level data bracket
that of the observations. While at the 1st model level, temperature and moisture are prognostic
variables of the general circulation equations (the integration of which alternates with a diagnostic
resolution of the diabatic and hydrological processes), the 2-m variables are interpolations between
the 1st level and the surface using gradient equations of the surface layer (Section 3.2 of Part IV,
330 physical processes of ECMWF IFS Cyc41r1 documentation). Vignon et al. [2016] show that the



surface layer where classical interpolation relationships are valid is often much shallower than 8 m in stable conditions at Dome C. The 2 m interpolated values probably encompass biases due to the interpolation formula and have to be considered carefully. The physics parameterizations for cold water condensation in the ECMWF model allow supersaturation to occur [Tompkins et al., 2007].
335 There are only 4 analyses steps per day, so ECMWF data are shown as dots on Figure 4 when the observations (48 data per day) are shown as continuous curves.

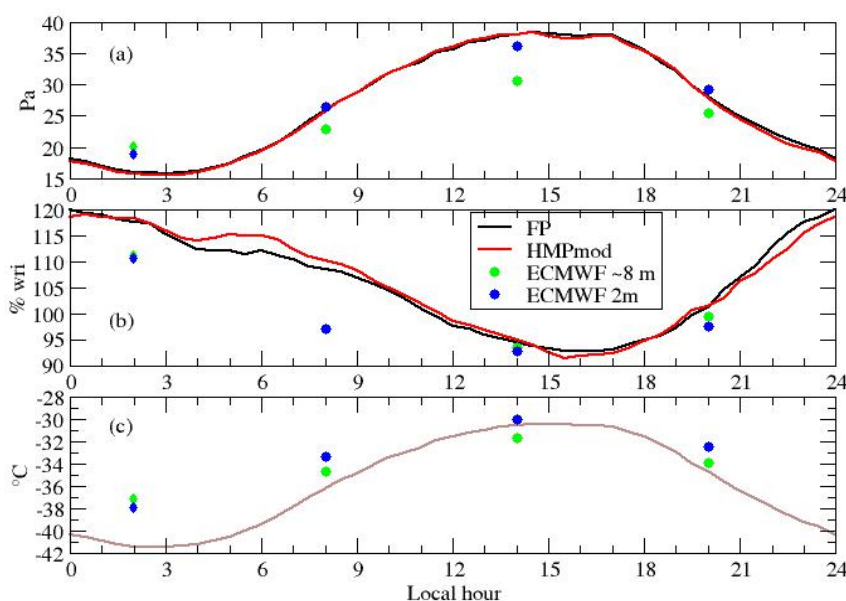


Figure 4: Mean Dec-Jan-Feb diurnal cycle of observed (FP and HMPmod) and analyzed (ECMWF, 340 2 m and 1st model level at ~8 m) water vapor partial pressure (a), relative humidity with respect to ice (b) and temperature (c). The reference temperature is that from the unmodified HMP (brown curve on plot (c)).

The ECMWF analyses overestimate night-time temperature and consequently underestimate the



345 amplitude of the diurnal cycle. The amplitude of the cycle of moisture partial pressure is also
underestimated but not as badly as could be expected considering a non linear relation between
temperature and saturation humidity. The model thus confirms a large diurnal change of magnitude
and sign of the surface turbulent flux of moisture. The surface atmosphere is expectedly moister,
and the vertical gradient and turbulent flux directed upward (surface sublimation) in the early
350 afternoon. It is downward (deposition) and very weak at night. Because of the temperature errors,
RH_i is less than observed at night, yet it is significantly larger than 100%. The analyzes reproduce
supersaturation at night and minimum RH in the early afternoon. While there are only 4 ECMWF
analyses per day, at synoptic times (dots on Figure 4), the time step of the MAR model is 6 minutes
only, which allows for a much more continuous comparison with the observations (Figure 5). Here,
355 a more recent version of the MAR model is used than in Genthon et al. [2013]. The model still uses
a parameterization for cold microphysics [Meyer et al. [1992] and produces large supersaturations,
actually too large compared to the observations in summer (Figure 5a). However, the model is now
significantly and consistently too warm (Figure 5b). It will be shown that the MAR model
significantly differs from the observations and ECMWF analyses in the rest of the year.

360

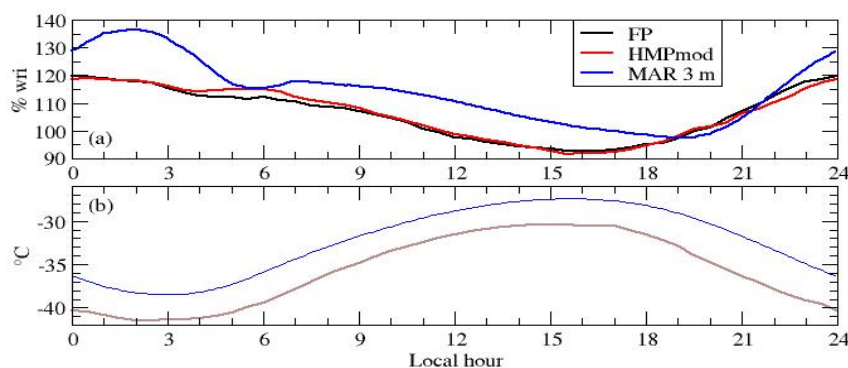




Figure 5: Mean Dec-Jan-Feb diurnal cycle of observed (FP and HMPmod for moisture, HMP for temperature) and MAR simulated RH_i (a) and air temperature (b), the brown curve being the observed as on Figure 4.

365

Figure 6 displays correlation plots of moisture reports from the unmodified (HMP) and modified (HMPmod) thin film capacitive sensors with respect to FP in summer. The direct correlations between water vapor pressures would be very high because humidity is largely controlled by temperature. Plotting deviations to the saturation vapor pressure, rather than the vapor pressure
370 itself, removes much of the temperature codependence effect and concentrates on the relative ability of the instruments to correctly measure moisture. The correlation between the regular HMP and FP is good below saturation but is obviously very poor above since the HMP fails to capture supersaturations. The correlation between HMPmod and FP reports is very high, above 0.97. The regression constant (the intercept) is 0.1 but the standard error on the constant is larger than 0.1. The
375 linear regression is thus not statistically different from a 1/1 one.

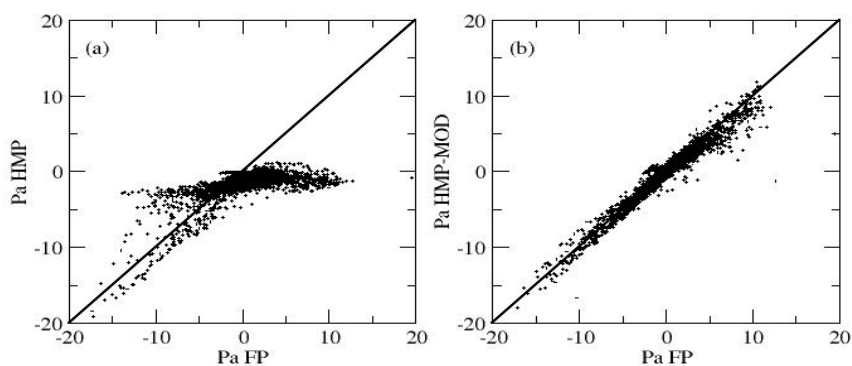


Figure 6: regression of anomaly to saturation vapor pressure from HMP ((a) and HMPmod (b) instruments against FP.



380 3.2 Annual variations and statistics

According to instrument reports, a strong diurnal cycle dominates the variability of atmospheric moisture in summer. The partial pressure is maximum in the early afternoon while RH_i peaks near local midnight (Figure 3) when it occasionally reach more than 150% (not shown). As the diurnal cycle variability progressively vanishes and is replaced by synoptic variability in the colder months, RH_i occasionally reaches values above 200%. Limiting the range to values between 50 – 150 % (more than 99% of HMPmod reports), Figure 7 displays the distribution functions of observed, ECMWF analyzed and MAR modeled RH_i.

390

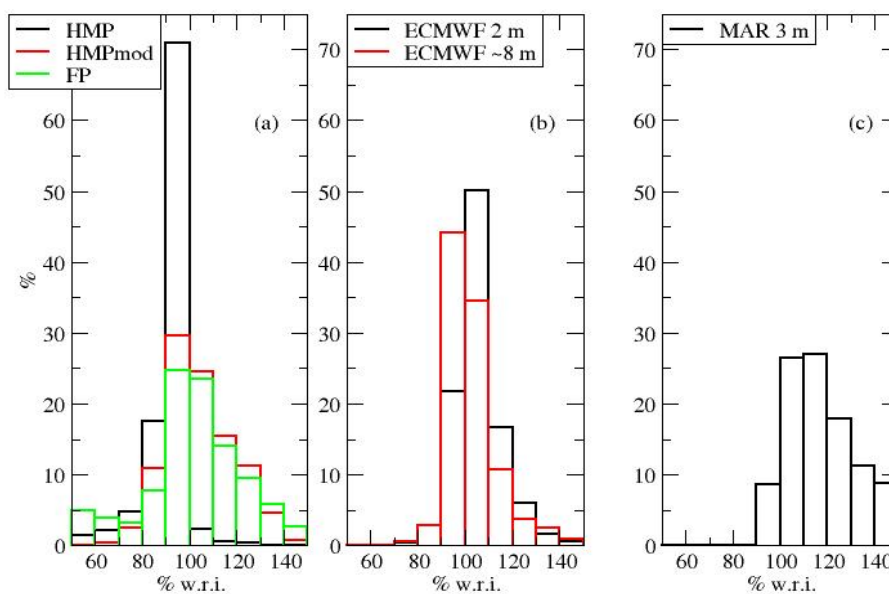


Figure 7: Observed (a), ECMWF analyzed (b) and MAR (c) distributions of Hi in 2015 for csases



of Rhi between 50 and 150%.

395 Although measurement uncertainties and uncertainties on conversions from relative humidity with
respect to liquid to RHi allow some occurrences above 100%, as expected the reports from HMP
peak near and hardly exceed the 100% ceiling. More than 50% of all reports between 50% and
150% are above 100% for HMPmod and FP, with a similar distribution for the 2 instruments. The 2
models are successful at reproducing very frequent occurrences of supersaturation, however their
400 distributions differ both with the observations and with each other. The MAR model is much more
often supersaturated than the observations report, and also than the ECMWF analyses. Further
analyses of these differences, comparing the respective cold physics parameterizations, tracking
possible contributions of temperature biases, is beyond the scope of the present study. However, this
result illustrates that because long series of consistent in situ observations are feasible at Dome C,
405 not only short term chronology but also the statistics of supersaturation can be observed and used to
exhibit differences in behavior of models and parameterizations of natural atmospheric
supersaturation.

Differences between models and between one or the other model and the observations are beyond
410 observation uncertainties. However, there are also significant differences between observations by
even the 2 modified hygrometers. There are more differences between the HMPmod and FP below
100% than above. Both the HMP155 and frost point hygrometer loose accuracy and sensitivity as
temperature is colder and/or water vapor partial pressure is less. Below -55°C, FP occasionally, and
more and more frequently as temperature gets colder, reports unrealistically low moisture content.
415 Figure 8 displays the regressions of water vapor partial pressure differences with saturation,
separately for partial pressure ranging between 2 and 5, 5 and 10, 10 and 20, and exceeding 20 Pa.
The correlation deteriorates, and the regression line increasingly deviates from 1 to 1, as the



moisture content decreases.

420 Obviously, the smallest moisture partial pressures occur when the temperature is coldest. The instruments show their limits during the coldest of the winter. Figure 9 displays the annual cycle of monthly averaged temperature and RH_i. HMP displays weak seasonal variability of RH_i compared to the other instruments. On the other hand, FP displays extreme seasonal variability with values reaching below 30% (beyond the plot scale on Figure 9) in winter. Such unrealistically low values, 425 at odd with the other instruments, reflect instrument limitation with very low moisture content. Limiting the analysis to cases of partial pressure of moisture above 2 Pa (dashed curves on Figure 9) excludes significant portions of the coldest parts of the winter records. This is reflected by monthly winter temperature more than 20°C warmer (Figure 9a). The fact that HMPmod reports are strongly increased suggests that this sensor also does not perform well at very low moisture levels.

430 Both HMPmod and FP show strong seasonal variability with monthly mean RH_i reaching 120% for HMPmod and exceeding 130% for FP. In both cases, the maximum monthly supersaturation is reached in early winter (April) and remains above 100% all year long, except in October for HMPmod when it is slightly below. Figure 10, same as Figure 7 but for partial pressure of moisture above 2 Pa only, confirms that in the surface atmosphere of Dome C, supersaturation is the norm 435 rather than an exception.

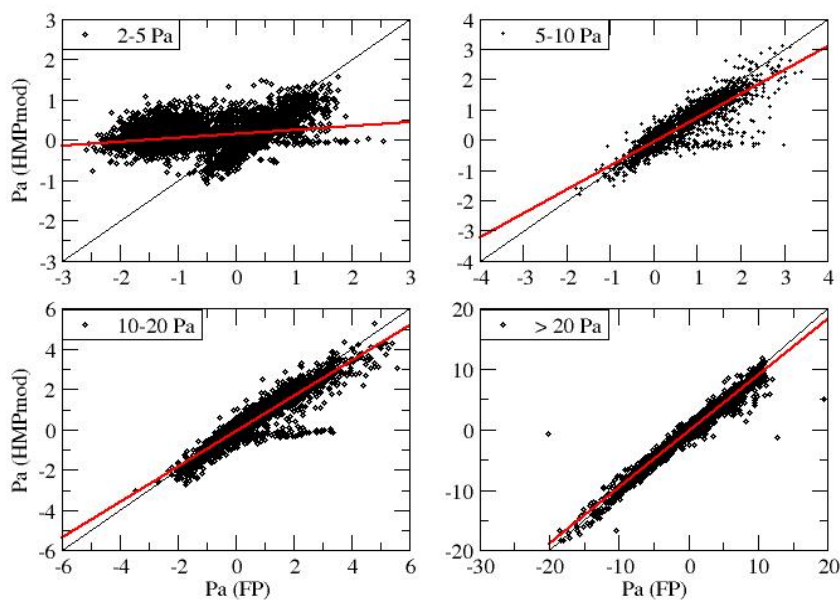


Figure 8: Regressions of partial pressure difference with saturation from HMPmod against FP,
440 depending on partial pressure range as indicated on the upper left corner of each plot. The black
line is the 1st bisector, the red line shows the linear regression.

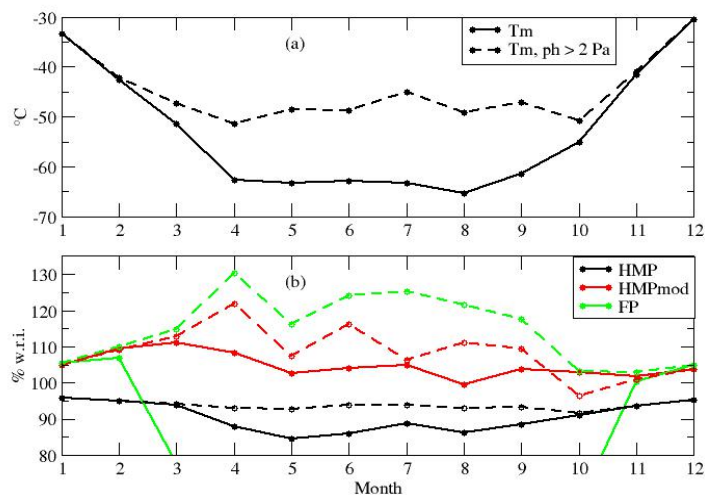


Figure 9: Seasonal variability of monthly-mean temperature (a) and RH_i (b) for all reports (solid
445 lines) and reports with moisture partial pressure above 2 Pa only (dashed lines). With all reports,
the curve for FP reaches below 30%, well beyond the plot scale (green solid line).

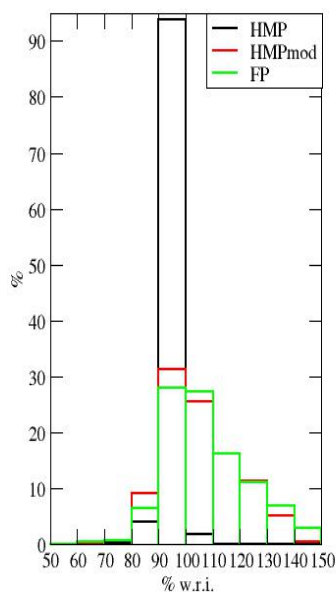


Figure 10, same as Figure 7a but for moisture partial pressure above 2 Pa only.

450

3.3 Impact on surface sublimation calculations

There are very few direct estimations of surface evaporation on the antarctic plateau. This is firstly because eddy correlation techniques use delicate high frequency sampling instruments such as sonic
455 anemometers which are hard to operate and maintain at the required level of performance in the extreme environment of the antarctic plateau. Moreover, due to the very low temperature, the water vapor content is very small and moisture sensors are not both fast and sensitive enough for such measurements in such conditions. For instance, Van As et al. [2005] report that eddy correlation measurements of latent heat flux were unsuccessful even in the summer at Kohonen station in
460 Antarctica ~3000 m above sea level. The authors thus resigned themselves to use bulk methods, a most widely employed approach in Antarctica [Stearns and Weidner, 1993]. However, bulk methods



are equally affected by measurement biases such as underestimation of water vapor content due to failure to measure supersaturation. The magnitude of the error can be estimated at Dome C by comparing bulk calculations using HMP and HMPmod water vapor reports.

465

The water vapor flux E from the snow surface (subscript 's') to the atmosphere is calculated using bulk-transfer formulae :

$$E = \rho C_Q U(z) [q_s - q(z)]$$

470

where ρ is the air density, $U(z)$ and $q(z)$ the wind speed and the specific humidity at the height z in the atmospheric surface layer and q_s the specific humidity at the surface, assuming saturation with respect to ice at the snow surface temperature. Here the wind speed and specific humidity are measured a $z \sim 3$ m above the surface, and the snow surface temperature is obtained from

475 measurement of the upwelling infrared radiation [Vignon et al., 2016] considering a snow emissivity of 0.99 [Brun et al., 2011]. C_Q is a bulk transfer coefficient which writes :

$$C_Q = \kappa^2 [\ln(z/z_0) - \psi_m(z/L)]^{-1} [\ln(z/z_{0q}) - \psi_q(z/L)]^{-1}$$

480 where κ is the Von Kármán's constant, z_0 et z_{0q} the roughness lengths for momentum and water vapor respectively and ψ_m and ψ_q are the corresponding surface-layer similarity stability functions.

Stability functions depend solely on the dimensionless height z/L , where L is the Monin-Obukhov length. The same 4 function schemes taken for stable conditions in Vignon et al. [2016] are tested here, and the functions from Hogström [1996] are selected for unstable conditions because they

485 provide reasonable results for momentum and heat fluxes at Dome C [Vignon et al, 2016] . L and thus C_Q are calculated with an iterative resolution of the Monin-Obukhov equations system. The



value of z_0 is the mean value reported by Vignon et al [2016] for Dome C (0.56 mm). The value of z_{0q} is difficult to estimate at Dome C because the very low vapor content of the atmosphere induces high uncertainties and because the scarcity of near-neutral conditions prevents an independent
490 selection of a scheme for the stability functions. Two different approaches are used. In the first one, $z_{0q}=z_0$ as in King et al [2001], whereas in the second one, z_{0q} is calculated with Andreas [1987] theoretical formula which, at Dome C, yields z_{0q} values lower than z_0 by approximately one order of magnitude. Uncertainties on flux calculations are estimated from the variance of results obtained with the different choices of stability functions and roughness length.

495

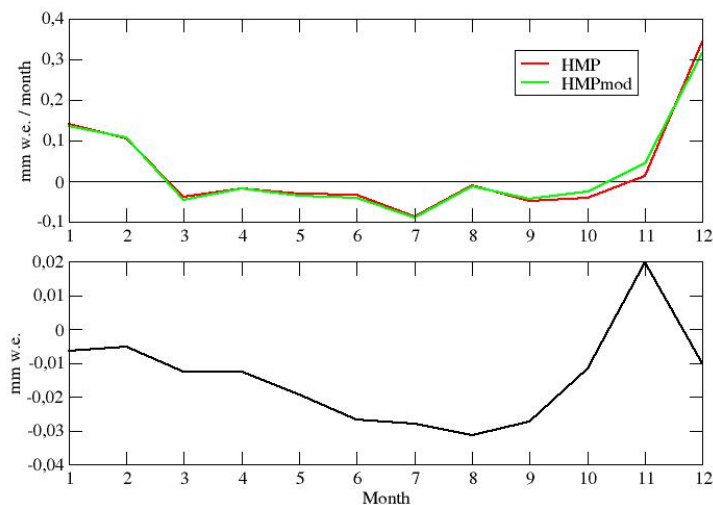


Figure 11. Annual march of the monthly vapor vapor flux at the surface according to HMP (red) and HMPmod (green), the black line showing 0, and cumulated difference (HMPmod – HMP, lower
500 plot).

Figure 11 shows the monthly seasonal and cumulated water flux calculated by the bulk method for



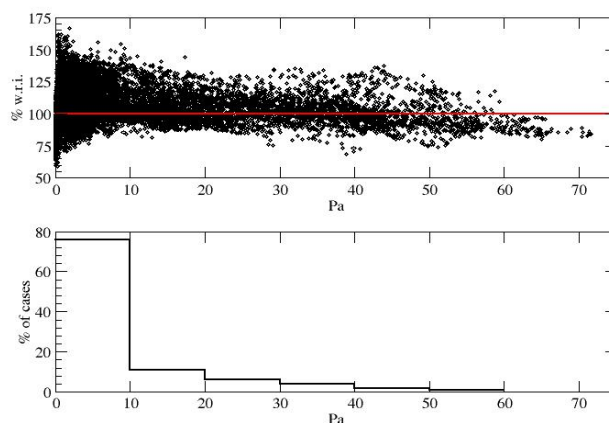
2015 using either HMP data or HMPmod reports. The flux is positive during the summer months indicating sublimation of snow while during winter months, the flux is negative indicating

505 condensation to the surface. Such seasonality is in agreement with that reported by King et al [2001] at Halley station, coastal Antarctica but at a latitude similar to that of Dome C. The positive summer values reflect the predominance of snow sublimation during the summer diurnal cycle [Genthon et al., 2013] because, in summer, the surface-atmosphere exchanges are larger during convective activity in the afternoon than in the night hours when the boundary layer becomes stable

510 (King et al. [2006], Vignon et al. [2016]). Integrated over the full year 2015, the net water vapor flux is 0.2763 cm w.e using HMPmod data and 0.2863 cm w.e using HMP data. These numbers can vary by as much as $\pm 100\%$ with the different choices of stability functions and roughness length values. They are very small anyway compared to the total surface water budget, given that the mean annual accumulation is about 2.5 cm water equivalent [Genthon et al., 2015]. However, a

515 mean positive evaporation agrees with Stearns and Weidner [1993] who, for other regions of Antarctica, conclude that the annual-mean net sublimation exceeds the annual-mean net deposition. In fact, Figure 11 shows very little difference between calculations made with HMP and HMPmod data: the impact of supersaturation on the water heat flux is thus very small. This is because supersaturations predominantly occur when the wind speed and thus turbulence is weak (not shown)

520 and under cold temperatures associated to low values of specific humidity (Figure 12). A possible contribution of blowing or drifting snow sublimation (King et al [2001], Frezzotti et al. [2004], Barral et al. [2014]) is not taken into account here.



525 *Figure 12 : According to HMPmod, relative humidity vs water vapor partial pressure, saturation*
shown by the red line (upper plot), and probability distribution function of RH_i above 105% with
respect to water vapor partial pressure (lower plot).

530

4. Discussion and conclusions

Major ice supersaturations are observed in the surface atmosphere of Dome C on the antarctic plateau in atmospheric temperature and moisture conditions close to those of the upper troposphere.

535 Fog formation can be observed in the field at temperatures for which heterogeneous freezing of the supercooled droplets would occur if ice nuclei were present. This suggests that the atmosphere is devoid of ice nuclei and that ice crystals, when present, are mostly formed by homogeneous freezing of supercooled droplets. This needs to be confirmed by detecting fog formation and analysing its properties. Meanwhile, to our knowledge it is the first time such strong

540 supersaturations (up to 200%) are observed in the natural surface atmosphere of the Earth.



Atmospheric supersaturations are frequent in the high troposphere where cirrus clouds form [Spichtinger et al., 2003]. On the other hand, atmospheric supersaturation is a very infrequent situation in the surface atmosphere because of the high concentration of aerosols and relatively mild temperatures which are both favorable to liquid and solid cloud formation. In this respect, the surface atmosphere of the high antarctic plateau is an exception. Because of the high albedo of snow and high elevation, the temperature is close to that of the high troposphere elsewhere even in summer. Long distance transport to such remote area is insufficient to import significant amounts of cloud and ice condensation nuclei even from the closest sources at the oceans, thus the possibility of strong and frequent supersaturation.

545

Because they are compact, light-weight and comparatively low cost, both to buy and to operate, solid state hygrometers (thin film capacitive sensors such as Vaisala's Humicap) are widely used to report atmospheric moisture from radiosondes or automatic weather stations. However, these sensors are subject to icing in supersaturated environment [Rädel and Shine, 2010] and require correction and/or adaptation. There are not many measurements of atmospheric moisture in Antarctica, and most including by the radiosondes are made using unadapted solid state sensors. The atmospheric humidity of the antarctic atmosphere where supersaturation is frequent is likely often underestimated from observations. Thus, the evaluation of meteorological and climate models from these data may be biased. Observations at Dome C using modified sensors to ensure that supersaturations can be sampled show that models that implement parameterizations of cold cloud microphysics intended to simulate cirrus clouds at high altitude qualitatively reproduce frequent supersaturations but fail with respect to the the statistics of supersaturation events. Moreover, they fail differently, both models producing too much supersaturation but one model simulating much more frequent occurrences of supersaturations than the other.

550
565



Estimations of the moisture budget of the antarctic atmosphere may be erroneous. Because it is comparatively undersampled by observation, studies of the antarctic atmosphere rely more than elsewhere on models and meteorological analyses. However, only models which microphysics parameterization account for supersaturation may, but not necessarily do, correctly reproduce

570 antarctic atmospheric moisture. One consequence of underestimating surface moisture, whether in observations or models not accounting for supersaturations, is likely that the surface turbulent moisture exchange (evaporation or sublimation) is wrong. Although the ground is made of thousands of meters of snow and ice slowly accumulated through millions of years, the antarctic plateau is one of the driest places on Earth. At Dome C, only about $\sim 3 \text{ kg m}^{-2}$ of water accumulates

575 each year [Genthon et al. 2015]. Out of this, the relative contribution of precipitation and evaporation is an open question. The direct measurement of both quantities is an unsolved challenge. For the turbulent fluxes, bulk and profile method parameterizations have their intrinsic limits because Monin-Obukov similarity theory requires empirical corrections functions which are not necessarily well established in very stable conditions [Vignon et al. 2016]. However, even the

580 best theory and best parameterization deployed based on this theory will poorly apply if the observations are wrong. The consequences are limited on the antarctic plateau though, because supersaturations are stronger and more frequent as temperature is lower, and moisture content and thus turbulent moisture flux smaller.

585 Finally, supersaturation has an important impact on the isotopic fractionation occurring during the formation of snow [Dansgaard 1964]. Indeed, supersaturation can only occur in condition with a small number of condensation nuclei during which the growth of the snowflakes is limited by the diffusion of water molecules. The difference in diffusivity of the different isotopes of water will therefore lead to kinetic fractionation. Jouzel and Merlivat [1984] have experimentally established

590 the impact of supersaturation on isotopic composition by a kinetic fractionation factor



$$\alpha_{kin} = \frac{S_i}{\alpha_{eq} D/D' (S_i - 1) + 1} .$$
 Here, S_i is the supersaturation, a_{eq} is the equilibrium fractionation,

D/D' is the diffusivity ratio between light and heavy isotope. This formulation is still used nowadays in most atmospheric models that include water isotopes (e.g. Risi et al. [2010]). In order to provide quantitative interpretation of ice core signal, it is important to include the impact of kinetic
595 fractionation which is significantly affecting the isotopic composition during the formation of the precipitation in the clouds, but also of the snow after the deposition. However, recent studies highlight important limitations of the Jouzel and Merlivat [1984] approach [Casado et al., 2016]. More importantly, all climatic models that include isotopic composition variables only estimate supersaturation from a parametrization from temperature and important discrepancies remain in this
600 parametrization. Although snow forms higher above the surface, our observations provide new constraints on ice supersaturation and will help improve these parameterizations.

Measurement of ice supersaturation as high as 200% in this very dry atmosphere is a game changer for understanding physical processes of the water cycle in Antarctica. The deployment of more
605 hygrometers that can measure supersaturation on the ~45-m meteorological mast is underway and will give more insights into water vapor fluxes. Comparisons to surface observations will also improve our understanding of dry deposition and formation of frost hoar, and possibly of diamond dust. These results open new possibilities of using stations in remote polar regions to study and understand phenomena normally occurring in clouds at several km of altitude.

610

Acknowledgements:

Support for field measurements was provided by the French polar institute IPEV through program CALVA (1013). Concordia station is jointly operated by the IPEV and PNRA. INSU provided
615 support through programs LEFE CLAPA and DEPHY2. Support by OSUG through observatory



program GLACIOCLIM is also acknowledged. The BSRN upwelling infrared radiation data which served to calculate the snow surface temperature were kindly provided by Christian Lanconelli, CNR ISAC. The research leading to these results has received funding from the European Research Council under the European Union's Seventh Framework Programme (FP7/2007-2013) / ERC grant 620 agreement n° [306045].

References:

Anderson, 1994. Mechanism for the behaviour of hydroactive materials in humidity sensors, *J. Atmos. Tech.*, 12, 662-667. 625

Andreas, E. L., 1987. A theory for scalar roughness and the scalar transfer coefficients over snow and sea ice. *Boundary-Lay. Meteorol.*, 38, 159-184.

630 Andreas, E. L., 2002. Parametrizing scalar transfer over snow and ice : A review. *J. Hydrometeorol.*, 3, 417-432.

Arthern, R. J., D. P. Winebrenner, D. G. Vaughan, 2006. Antarctic snow accumulation mapped using polarization of 4.3-cm wavelength microwave emission. *J. Geophys. Res.* 111, D06107, 635 DOI:10.1029/2004JD005667.

Barral, H., Genthon C., Trouvilliez A., Brun C., and Amory C., 2014. Blowing snow in coastal Adélie Land, Antarctica : three atmospheric moisture issues, *The Cryosphere*, 8, 1905–1919, doi:10.5194/tc-8-1905-2014.

640



- Brun, E., D. Six, G. Picard, V. Vionnet, L. Arnaud, E. Bazile, A. Boone, O. Bouchard, C. Genthon, V. Guidard, P. Le Moigne, F. Rabier, and Y. Seity, 2011. Snow-atmosphere coupled simulation at Dome C, Antarctica, *J. Glaciol.* **57**,721-736
- 645 Casado, M., Cauquoin, A., Landais, A., Israel, D., Orsi, A., Pangui, E., Landsberg, J., Kerstel, E., Prie, F. and Doussin, J.-F., 2016. Experimental determination and theoretical framework of kinetic fractionation at the water vapour–ice interface at low temperature. *Geochimica et Cosmochimica Acta* **174**, 54-69.
- 650 Dansgaard, W., 1964. Stable isotopes in precipitation. *Tellus* **16**, 436-468.
- Frezzotti, M., Pourchet, M., Flora O., Gandolfi, S., Gay, M., Urbini, S., Vincent, C., Becagli, S., Gragnani, R., Proposito, M., Severei, M., Traversi, R., Udisti, R. and Fily, M., 2004, New estimation of precipitation and surface sublimation in East Antarctica from snow accumulation
655 measurements. *Clim. Dyn.*, **23**, 803-813.
- Gallée, H. and Gorodetskaya, I. V. (2010). Validation of a limited area model over Dome C, Antarctic Plateau, during winter. *Climate Dynamics*, **34**:61–72.
- 660 Genthon, C., M. S. Town, D. Six, V. Favier, S. Argentini, and A. Pellegrini, 2010. Meteorological atmospheric boundary layer measurements and ECMWF analyses during summer at Dome C, Antarctica, *J. Geophys. Res.* **115**, D05104, doi:10.1029/2009JD012741.
- 665 Genthon, C., D. Six, V. Favier, M. Lazzara, L. Keller, 2011. Atmospheric temperature measurement biases on the Antarctic plateau, *J. Atm. Oceanic Technol.*, DOI 10.1175/JTECH-D-11-00095.1 **28**, No. 12, 1598-1605.



Genthon C., Six D., Gallée H., Grigioni P., and Pellegrini A., 2013. Two years of atmospheric boundary layer observations on a 45-m tower at Dome C on the Antarctic plateau, *J. Geophys. Res.* 670 *Atmos.*, 118, 3218–3232, doi:[10.1002/jgrd.50128](https://doi.org/10.1002/jgrd.50128).

Genthon, C., D. Six, C. Scarchilli, V. Giardini, M. Frezzotti, 2015. Meteorological and snow accumulation gradients across dome C, east Antarctic plateau, *Int. J. Clim.*, 36, 455-466, DOI: [10.1002/joc.4362](https://doi.org/10.1002/joc.4362)

675

Goff J. A., and S. Gratch, 1945. Thermodynamics properties of moist air, *Tans. Amer. Soc. Heat. Vent. Eng.*, 51, 125-157.

Jouzel J., Lorius C., Petit J. R., Genthon C., Barkov N. I., Korotkevitch Y. S., and Kotlyakov V. M., 680 1987. Vostok ice core: A continuous isotope temperature record over the last climatic cycle (160000 years), *Nature* **329**, 403-408.

Jouzel, J. and Merlivat, L., 1984. Deuterium and oxygen 18 in precipitation: Modeling of the isotopic effects during snow formation. *J. Geophys. Res.* 89, 11749-11757.

685

Kämpfer N (ed), 2013. Monitoring Atmospheric Water Vapor. Ground-based Remote Sensing and In-situ Methods, ISSI Scientific Report Series, 10, Springer, New York.

King, J. C. and Anderson, P.S., 1999, A humidity climatology for Halley, Antarctica, based on frost- 690 point hygrometer measurements. *Antarctic Science*, 11, 100-104



- King, J.C., Anderson, P.S. and Mann, G.W., 2001. The seasonal cycle of sublimation at Halley, Antarctica. *J. Glaciology*, 47, 56
- 695 King, J.C., Argentini, S. A. and Anderson, P. S., 2006. Contrast between the summertime surface energy balance and boundary layer structure at Dome C and Halley stations, Antarctica. *J. Geophys. Res.*, 111, D02105
- Meyer, M. P., P. J. Demott, and W. R. Cotton, 1992. New primary ice nucleation parameterizations
700 in an explicit cloud model, *J. Appl. Meteorol.*, 31, 708–721.
- Rädel, G., and K. P. Shine, 2010. Validating ECMWF forecasts for occurrences of ice supersaturation using visual observations of persistent contrails and radiosonde measurements over England, *Q. J. R. Meteorol. Soc.*, 136, 1723-1732.
- 705
- Risi, C., Bony, S., Vimeux, F. and Jouzel, J. (2010) Water-stable isotopes in the LMDZ4 general circulation model: Model evaluation for present-day and past climates and applications to climatic interpretations of tropical isotopic records. *J. Geophys. Res.* 115, D12118.
- 710 Schwerdtfeger, W., 1970. The climate of the Antarctic, Vol. 14, S. Orvig Ed., World survey of climatology, H. E. Landsberg Ed. Elsevier, 253-355.
- Spichtinger, P., Gierens, K., Read, W.: The global distribution of ice-supersaturated regions as seen by the microwave limb sounder. *Q. J. R. Meteorol. Soc.* 129, 3391–3410 (2003). doi:
715 10.1256/qj.02.141



Spichtinger, P., K. Gierens¹, H. G. J. Smit², J. Ovarlez³, and J.-F. Gayet⁴, 2004. On the distribution of relative humidity in cirrus clouds, *Atmos. Chem. Phys.*, 4, 639–647.

720 Stearns, C. R. and Weidner, G. A., 1993, Sensible and Latent heat flux estimates in Antarctica. Antarctic research series, 61, 109-138.

Tompkins, A. M., Gierens, K. and Rädcl, G., 2007. Ice supersaturation in the ECMWF integrated forecast system. *Q. J. R. Meteorol. Soc.*, 133, 53–63.

725

Van As, D., van den Broeke, M., Reijmer, C., and van de Wal,, M., 2005. The summer surface energy balance of the high antarctic plateau, *Boundary-Layer Meteorol.* 115, 289-317.

Vignon, E., Genthon C., Barral, H., Amory, C., Picard, G., Gallée, H., Casasanta, G. and Argentini,

730 S., 2016. Momentum and heat flux parametrization at Dome C, Antarctica : a sensitivity study, *Boundary-Lay. Meteorol.*, in press.